Field-induced spin orders in monoclinic CoV_2O_6

Field-induced spin orders in monoclinic CoV_2O_6

Mikael Markkula, Angel M. Arévalo-López, and J. Paul Attfield*
Centre for Science at Extreme Conditions and School of Chemistry, University of Edinburgh, Mayfield Road, Edinburgh EH9 3JZ, United Kingdom
(Received 7 August 2012; published 1 October 2012)

Spin-ordered structures of monoclinic brannerite-type CoV_2O_6 have been determined from neutron diffraction data recorded at 2 K in applied magnetic fields of 0, 2.5, and 5.0 T. Three collinear magnetic phases were observed as field increases: an antiferromagnetic state with propagation vector (0 1 ½), a ferrimagnetic (⅓ 1 ⅓) phase, and a (0 0 0) ferromagnetic order. Co^{2+} moments of 4.4–5.0 μ_B have a large orbital component and are aligned close to the *c*-axis direction in all cases. Spin-lattice coupling leads to a magnetostriction and volume expansion as field increases. The ferrimagnetic phase accounts for the previously reported 1/3-magnetization plateau, and demonstrates that monoclinic CoV_2O_6 behaves as an accidental triangular antiferromagnetic lattice in which further frustrated orders may be accessible.

DOI: 10.1103/PhysRevB.86.134401 PACS number(s): 75.25.−j, 75.47.Lx, 75.50.Gg

Low-dimensional lattices of Ising spin ions are of great interest for the variety of quantum magnetic ground states and unusual excitations that may emerge, such as propagation of domain walls (solitons) that can occur when neighboring chains are weakly coupled together. Phenomena such as metamagnetism and intermediate magnetization plateaus, which are more commonly observed in frustrated triangular systems,[1–3] have recently been reported in the brannerite-type material CoV_2O_6 which is found in monoclinic (α) and triclinic (γ) forms, both containing quasi-one-dimensional ferromagnetic chains of high-spin Co^{2+} ions.[4–12] Large single-ion anisotropy leads to Ising-type behavior of the octahedrally coordinated high-spin Co^{2+} $S = 3/2$ spins, while the $3d^0$ V^{5+} ions act as nonmagnetic spacers between chains. Both VO_6 octahedra and VO_4 tetrahedra are found in the triclinic phase, where the chains contain two symmetry-inequivalent Co sites in a 1:2 ratio. However, monoclinic CoV_2O_6 is isostructural with the aristotype mineral brannerite UTi_2O_6, and contains only VO_6 octahedra with all Co sites equivalent.

Both monoclinic and triclinic CoV_2O_6 display long-range antiferromagnetic transitions in zero applied magnetic field, at Néel temperatures of $T_N = 15$ and 7 K, respectively. They have similar magnetic phase diagrams below T_N, with a field-induced transition to a 1/3- (of saturated) magnetization plateau and a further metamagnetic transition to the fully saturated ferromagnetic phase.[7–10] An inelastic neutron scattering study of the triclinic phase revealed deconfined soliton excitations above T_N instead of the static spin reversals expected for ferromagnetic Ising spin chains.[9] A ladder of states due to the confining influence of spin order was found below T_N, and weak confinement effects in the critical region may correspond to a crossover between two- and three-dimensional magnetic orders.

Powder neutron diffraction showed that the zero-field spin order in triclinic CoV_2O_6 is incommensurate, and the full spin structure was not reported.[9] However, a simple commensurate antiferromagnetic order was discovered in the monoclinic form (details are shown later),[11] in keeping with several predictions.[10,12] Models for the spin order in the 1/3-magnetization phase have also been predicted in several recent papers.[10–12] A Wang-Landau simulation in Ref. 12, treating the monoclinic lattice of CoV_2O_6 as a distorted triangular system, showed that the 1/3-magnetization plateau derives from the same field-induced ferrimagnetic state as observed in a regular frustrated antiferromagnetic triangular system, but with a different behavior of the critical fields due to the relaxation of magnetic frustration by anisotropy. To clarify the high-field behavior of monoclinic CoV_2O_6, we have carried out a high-field powder neutron diffraction study, and we report here the experimental spin structures of the 1/3-magnetization and the fully saturated phases.

The preparation of the single-phase 3-g sample of polycrystalline CoV_2O_6 used for this study is described in Ref. 11. Powder neutron diffraction patterns were measured using the long-wavelength, time-of-flight neutron diffractometer WISH at the ISIS spallation source UK. The powder was cold pressed into a vanadium sample can and data were collected at 2 K at a 0 → 2.5 T → 5.0 T → 0 sequence of applied magnetic field strengths. The final zero-field data were recorded to check for any alignment of sample grains by the applied fields. A small degree of field texturing was evident by comparing the initial and final zero-field data sets (Fig. 1). This does not affect the identification of the high-field states, but does lead to refinement uncertainties such as in the directions of ordered Co moments in the *ac* plane noted in the following. Data were normalized using the MANTIDPLOT program,[13] which was also used for creating the figures, and crystal and magnetic structures were refined using the GSAS software package.[14]

The changes in magnetic neutron diffraction intensities of CoV_2O_6 at 2 K with applied magnetic field are shown in Fig. 1. In zero field, all of the magnetic *hkl* Bragg peaks have half-integer values of *l* when indexed on the nuclear cell of the crystal structure which has space group symmetry $C2/m$. This condition is equivalent to applying propagation vector (0 1 ½) [or (1 0 ½)] to the *C*-centered monoclinic cell, or (0 0 ½) to a primitive cell with the same lattice parameters. The spin structure, shown in Fig. 2(a), is antiferromagnetic with equal numbers of spin-up and -down ferromagnetic chains.[11] Each chain is coupled antiferromagnetically to four neighbors and ferromagnetically to two in the quasitriangular *ac*-plane packing of the brannerite structure.

A 1/3-magnetization plateau between 1.9 and 3.2 T was previously reported for monoclinic CoV_2O_6.[7,8] When a field of 2.5 T is applied, the neutron intensities due to the

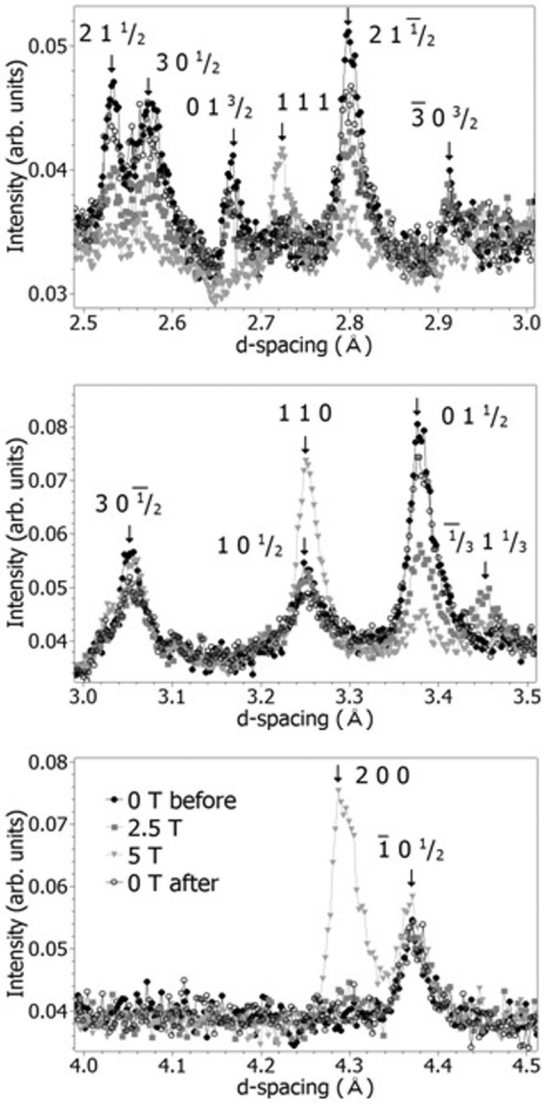

FIG. 1. Magnetic neutron powder diffraction peaks from monoclinic CoV_2O_6 at 2 K for the 0 → 2.5 T → 5.0 T → 0 sequence of applied magnetic fields. Magnetic peaks are labeled with *hkl* indices relative to the nuclear cell; peaks with half-integral/third-integral/integral values of *l* originate from the antiferromagnetic/ 1/3-magnetization/ferromagnetic magnetic phases shown respectively in Figs. 2(a)–2(c).

antiferromagnetic ground state are suppressed, and a prominent new peak indexed as $\bar{1}/3\ 1\ 1/3$ on the $C2/m$ cell appears. This is in agreement with a predicted ferrimagnetic model for the 1/3-magnetization phase [Fig. 2(b)].[11] Although the ($^{-1}/_3$ 1 $^1/_3$) propagation vector suggests that the magnetic cell is nine times larger than the nuclear $C2/m$ cell, a smaller cell with vectors $\boldsymbol{a} = \boldsymbol{a}_n + \boldsymbol{c}_n$, $\boldsymbol{b} = \boldsymbol{b}_n$, and $\boldsymbol{c} = 3\boldsymbol{c}_n$ can be used, where $\boldsymbol{a}_n,\boldsymbol{b}_n,\boldsymbol{c}_n$ are the nuclear cell vectors. This has three times the volume of the nuclear cell, and corresponds to a quasiorthorhombic triple superstructure of the quasihexagonal brannerite subcell.[11] There are two spin-up ferromagnetic chains for every one spin-down chain (where spin-up is taken to be the majority-spin direction), giving the exact resultant 1/3 magnetization. The majority-spin chains have three parallel and three antiparallel neighbors in the quasihexagonal packing,

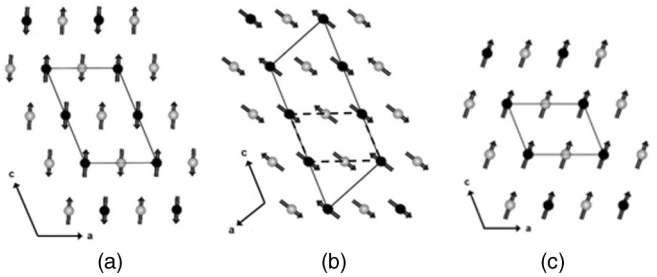

FIG. 2. Fitted models for (a) the zero-field antiferromagnetic, (b) the ferrimagnetic 1/3-magnetization, and (c) the fully saturated ferromagnetic phases of CoV_2O_6 at 2 K. Co^{2+} spins are parallel to the (010) plane in all phases. Majority up spins point towards the bottom right corner in (b). Magnetic unit cells and axes are shown, and the structural cell is also indicated by broken lines on (b) for comparison. The Co^{2+} spin chains are perpendicular to the (010) plane and Co atoms at heights $y = 0$ or 1/2 are shown with dark or light fill.

while the minority-spin chains have six antiparallel neighbors [Fig. 2(b)].

In an applied field of 5 T, above the upper limit for the 1/3-magnetization plateau, the magnetic peaks from both the antiferromagnetic and the ferrimagnetic superstructures are suppressed, and additional intensities at positions of nuclear reflections such as 110, 111, and 200 are observed. These correspond to a simple ferromagnetic order of spin chains with propagation vector (0 0 0), as shown in Fig. 2(c).

The crystal structure of monoclinic CoV_2O_6 and the above spin structures were fitted to the neutron diffraction data at the different field strengths (Fig. 3). Lattice parameters and atomic positions for the magnetic phases were constrained to those of the nuclear phase. Co-existing magnetic phases were observed (antiferromagnetic and 1/3-magnetization phases at 2.5 T; all three spin-ordered phases at 5 T) and fitted to the high-field data. This reflects the use of an unaligned powder of magnetically anisotropic CoV_2O_6.

The refinements of the three magnetic phases showed that the Co^{2+} magnetic moments always have collinear order in the *ac* plane, close to the *c* direction which was reported as the easy axis from single-crystal magnetization studies.[7] No spin components parallel to ***b*** were observed. Variations between moment directions in the three refined structures (Fig. 2) probably reflect refinement errors due to slight field texturing of the sample [see Figs. 1 and 3(b)]. Single-crystal neutron data would be needed to confirm accurate moment directions. The magnitudes of the ordered moments from the 0-, 2.5-, and 5.0-T data fits were 4.4(1), 4.4(1), and 5.0(2) μ_B, respectively. These are consistent with the 4.8 μ_B value reported in a previous study of the zero-field structure.[11] The ordered Co^{2+} moments in monoclinic CoV_2O_6 significantly exceed the ideal spin-only value of 3 μ_B, evidencing a strong orbital contribution.

The changes in 2-K lattice parameters (Table I) evidence a magnetostriction in CoV_2O_6 as the spin orders evolve. Figure 4 shows the percentage changes in cell parameters and volume. The overall volume increase as magnetic field increases from 0 to 5 T is mainly driven by an expansion of the ferromagnetic spin chains parallel to ***b***, with smaller changes in the *ac* plane. These displacements probably reflect small changes in

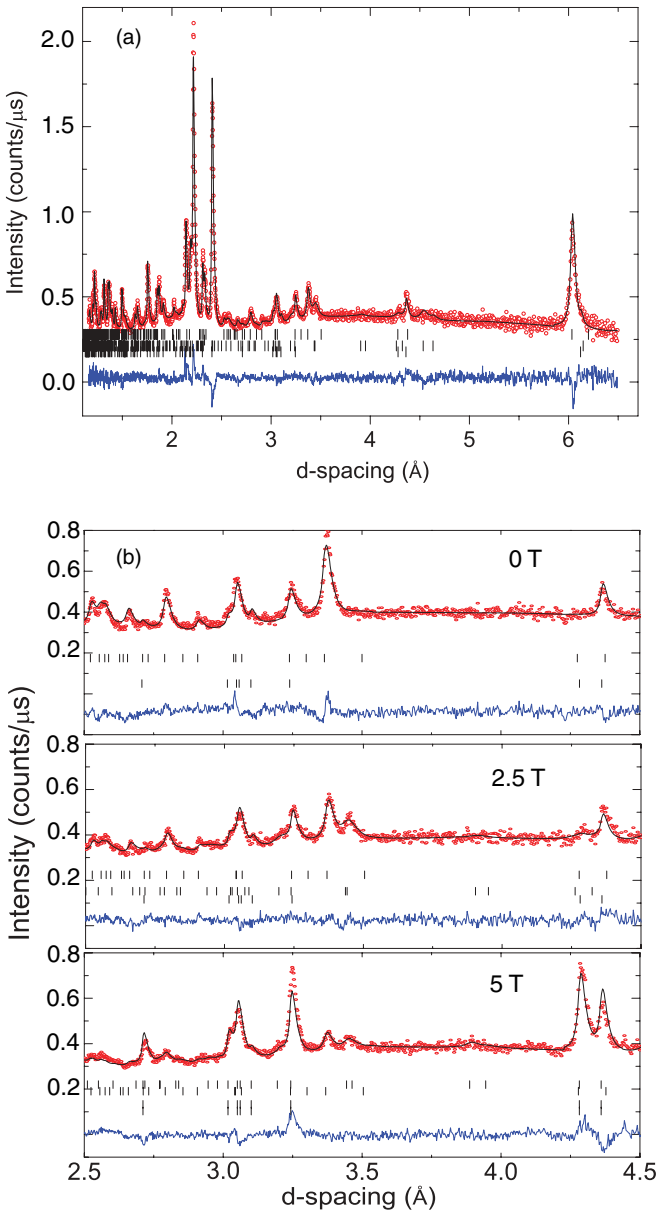

FIG. 3. (Color online) Fits to neutron profiles from the 90° detector bank of diffractometer WISH for CoV_2O_6 at 2 K and variable magnetic field strengths. (a) Fit to the entire profile at 2.5 T. Bragg reflection markers correspond to the nuclear phase, the 1/3-magnetization ferrimagnetic spin structure, aluminum (from the collimator), and the antiferromagnetic phase, respectively, from bottom to top. The overall fitting residuals were reduced-$\chi^2 = 3.70$, weighted-profile residual $R_{wp} = 0.056$, profile residual $R_p = 0.039$. (b) Fits to the prominent magnetic peaks in the range of Fig. 1 for applied fields of 0, 2.5, and 5.0 T. Discrepancies due to field texturing of the sample are evident in the 5.0-T fit.

the geometries of the Co-O-Co and Co-O-V-O-Co pathways that mediate the superexchange interactions. However, the refined atomic coordinates did not show any field variation, or differ significantly from those previously reported at 4 K.[11] A magnetostriction as CoV_2O_6 is cooled through the Néel transition was also reported in Ref. 11.

Ferromagnetic Co^{2+} chains are present in the three spin-ordered phases of monoclinic CoV_2O_6 with moments confined

TABLE I. Refined lattice parameters and volume for the $C2/m$ unit cell of monoclinic CoV_2O_6 at 2 K as a function of magnetic field strength.

H (T)	0	2.5	5.0
a (Å)	9.2442(5)	9.2368(5)	9.2391(5)
b (Å)	3.5000(1)	3.5044(1)	3.5044(1)
c (Å)	6.5997(3)	6.6036(3)	6.6055(3)
β (°)	112.092(5)	112.039(4)	112.030(4)
V (Å^3)	197.85(2)	198.13(2)	198.26(2)

to the ac plane. Strong spin-orbit (and hence spin-lattice) coupling is evidenced by the large values of the ordered moment, and magnetostrictions as spin order varies with field or temperature. Although the brannerite structure is not derived from a hexagonal lattice type, and Co atoms are present at two different positions in the chain direction (indicated by dark or light fill on Fig. 2), the observed interchain spin orders in the ac plane are typical for a quasitriangular antiferromagnetic lattice. The triangles of interchain couplings are parallel to [100], [001], and [101] directions, using the lattice vectors of the antiferromagnetic phase in Fig. 2(a) throughout for convenience. In the antiferromagnetic zero-field phase, spin chains are antiparallel to neighbors in the [100] and [001] directions, but parallel along [101]. The ferrimagnetic 1/3-magnetization phase has antiparallel couplings in the [100] direction but up-down-up repeat sequences in the [001] and [101] directions. These orders are consistent with antiferromagnetic interaction magnitudes $J_{100} > J_{001} > J_{101}$ on the triangular lattice, with frustration of the weakest J_{101} interactions in the zero-field phase.

A recent simulation of the phase diagram for geometrically frustrated triangular antiferromagnets[15] has shown that other collinear intermediate-magnetization phases may be realized in addition to the 1/3-magnetization order, and several of these have been observed in the delafossite $CuFeO_2$.[16] Reported magnetization measurements[8] for monoclinic CoV_2O_6 at low

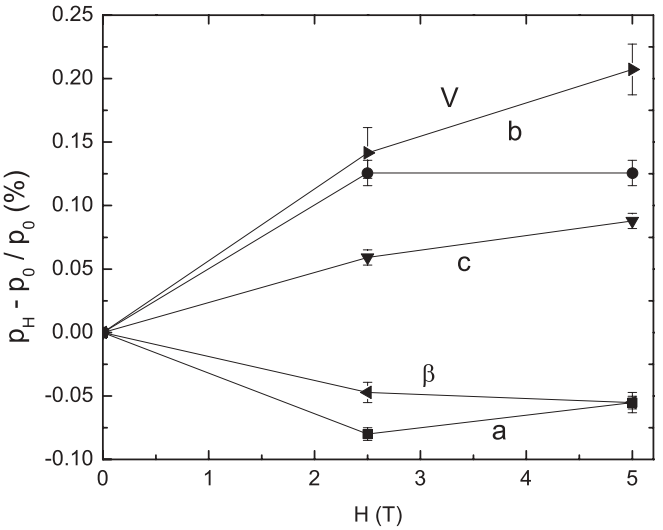

FIG. 4. Field-induced changes in the lattice parameters ($p \equiv a$, b, c, β, or V; subscripts refer to applied magnetic field) of CoV_2O_6 at 2 K.

temperatures (below 5 K) showed, in addition to the 1/3-magnetization plateau, steps at 1/5 and 2/5 of saturation that may correspond to additional phases with more complex orders of spin-up and -down chains. A collinear 1/5-magnetization state with a large stability domain is shown in the computed phase diagram,[15] although a 2/5 state is not featured. Hence, it appears likely that new field-induced states of the frustrated triangular antiferromagnetic lattice may be accessible in monoclinic CoV_2O_6.

In conclusion, this study has shown that the 1/3-magnetization phase in monoclinic CoV_2O_6 arises from the accidental near equivalence of antiferromagnetic interchain exchange interactions that lead to spin orders typical of a frustrated two-dimensional triangular lattice. Co^{2+} moments have a large orbital component and are collinearly ordered, near parallel to the *c* axis, in the antiferromagnetic, 1/3-magnetization, and fully saturated ferromagnetic phases. Spin-lattice coupling leads to a magnetostriction and volume expansion as field increases. Further ordered phases such as a 1/5-magnetization state may be observable at other field strengths in monoclinic CoV_2O_6.

We acknowledge EPRSC and the Leverhulme Trust for support. We also thank STFC for access to neutron diffraction facilities at ISIS and P. Manuel for assistance with the data collection.

*j.p.attfield@ed.ac.uk

[1] M. Hase, M. Kohno, H. Kitazawa, N. Tsujii, O. Suzuki, K. Ozawa, G. Kido, M. Imai, and X. Hu, Phys. Rev. B **73**, 104419 (2006).

[2] H. Kikuchi, Y. Fujii, M. Chiba, S. Mitsudo, T. Idehara, T. Tonegawa, K. Okamoto, T. Sakai, T. Kuwai, and H. Ohta, Phys. Rev. Lett. **94**, 227201 (2005).

[3] N. Bellido, C. Simon, and A. Maignan, Phys. Rev. B **77**, 054430 (2008).

[4] B. Jasper-Tonnies and H. Muller-Buschbaum, Z. Anorg. Allg. Chem. **508**, 7 (1984).

[5] K. Mocala and J. Ziolkowski, J. Solid State Chem. **69**, 299 (1987).

[6] M. Belaiche, M. Bakhache, M. Drillon, A. Derrory, and S. Vilminot, Phys. B (Amsterdam) **305**, 270 (2001).

[7] Z. He, J. Yamaura, Y. Ueda, and W. Cheng, J. Am. Chem. Soc. **131**, 7554 (2009).

[8] M. Lenertz, J. Alaria, D. Stoeffler, S. Colis, and A. Dinia, J. Phys. Chem. C **115**, 17190 (2011).

[9] S. A. J. Kimber, H. Mutka, T. Chatterji, T. Hofmann, P. F. Henry, H. N. Bordallo, D. N. Argyriou, and J. P. Attfield, Phys. Rev. B **84**, 104425 (2011).

[10] K. Singh, A. Maignan, D. Pelloquin, O. Perez, and Ch. Simon, J. Mater. Chem. **22**, 6436 (2012).

[11] M. Markkula, A. M. Arevalo-Lopez, and J. P. Attfield, J. Solid State Chem. **192**, 390 (2012).

[12] X. Yao, J. Phys. Chem. A **116**, 2278 (2012).

[13] http://www.mantidproject.org/Main_Page

[14] A. C. Larson and R. B. Von Dreele, "General Structure Analysis System (GSAS)", Los Alamos National Laboratory Report LAUR 86-748 (1994).

[15] R. S. Fishman, Phys. Rev. Lett. **106**, 037206 (2011).

[16] S. Kanetsuki, S. Mitsuda, T. Nakajima, D. Anazawa, H. A. Katori, and K. Prokes, J. Phys.: Condens. Matter **19**, 145244 (2007).